Universidad de La Laguna

Master en Biomedicina

Trabajo Fin de Máster

Curso 2019-2020

The Role of SGK1 in Regulating Hepatocyte Energy Metabolism.

Presentado por Cynthia Jorge Concepción

Directores: Diego Álvarez de la Rosa

Silvia Velázquez García

El Dr. Diego Álvarez de la Rosa Rodríguez y la Dra. Silvia Velázquez García, coordinador e integrante respectivamente de la línea de investigación Fisiopatología de los Mineralocorticoides, integrada en el Programa de Doctorado en Ciencias de la Salud de la Universidad de La Laguna

CERTIFICAN

- Que el trabajo de fin de Master (TFM) titulado "**The Role of SGK1 in regulating hepatocyte energy metabolism"** ha sido realizado bajo mi supervisión por Dª Cynthia Jorge Concepción, matriculada en el Máster en Biomedicina, durante el curso académico 2019-2020.

- Que una vez revisada la memoria final del TFM, damos nuestro consentimiento para ser presentado a la evaluación (lectura y defensa) por el Tribunal designado por la Comisión Académica de la Titulación.

Para que conste, firmo el presente certificado en La Laguna a 2 de Julio de 2018

Dr. Diego Álvarez de la Rosa Rodríguez   Dra. Silvia Velázquez García

INDEX

ABBREVIATIONS

AKT – Serine/threonine kinase known as Protein Kinase B
AMPK – Activated protein kinase
ATP – Adenosine Triphosphate
BAC - Bacterial artificial chromosome
BK/ERK5 - Bone marrow kinase/extra - cellular signal-regulated kinase 5
CreaT - Creatine Transporter
DMEM – Dulbecco's Modified Eagle Medium.
DOCA - Deoxycorticosterone acetate
ECM – Extracellular Matrix
ENaC – Sodium Epithelial Channel
Foxo3a – Forkhead box O3a
FSH – Follicle-stimulating Hormone
G3P – Glyceraldehyde-3-phosphate
G6P – Glucose 6-Phosphatase
GAPDH – Glyceraldehyde 3-phosphate Dehydrogenase
GLUT 1 – Glucose Transporter 1
GSK3 – Glycogen Synthase Kinase-3
GTT – Glucose Tolerance Test
HFD – High-fat Diet
HGF – Hepatic Growth Factor
HGP – Hepatic Glucose Production
HM – Hydrophobic motif.
HMM – Hepatocyte Maintenance Medium
IGF-1 – Insulin-like Growth Factor 1
IRS – Insulin Receptor Substrate
ITT – Insulin Tolerance Test
MetS – Metabolic Syndrome
MR – Mineralocorticoid Receptor
mTORC2 - Mammalian Target of Rapamycin Complex 2
NAFL - Non-alcoholic Fatty Liver
Nedd4-2 - Ubiquitin Protein Ligase Nedd4-2
PDH - Pyruvate Dehydrogenase
PDK – Phosphoinositide-dependent kinase
PH – Pleckstrin homology domain
PI3K – Phosphatidylinositol-3-kinase
PIP3 – 3phophonisite
PKB – Protein kinase B
PPP – Pentose Phosphate Pathway
PTT – Pyruvate Tolerance Test
RSK – Ribosomal S6 Kinase
S6Ks - S6 Kinases
SGK1 - Serum and Glucocorticoid Kinase 1
SGLT1- Sodium Glucose Transport Protein 1
SCD- Standard Chow Diet
TCA cycle - Tricarboxylic Acid cycle
Tg – Transgenic
TGF- β – Transforming Growth Factor β
TBS-T – Tris Buffered Saline with Tween.

ABSTRACT

The importance of the serum and glucocorticoid kinase 1 (SGK1) in the regulation of energy metabolism has become apparent in the last few years. This serine/threonine protein kinase is part of the insulin signaling pathway and is as a transcriptional target of glucocorticoids. It appears to play an important role in regulating insulin sensitivity, glucose uptake and glucose metabolism and fat deposition. In addition, it is also a target of mineralocorticoids, and promotes kidney Na^+ reabsorption, controlling blood pressure. Excess SGK1 activity has been proposed to be a risk factor for the development of obesity and Metabolic Syndrome (MetS). Previous studies conducted in our laboratory led us to hypothesized that SGK1 activity increases glucose production by activating gluconeogenesis, which in turn contributes to the development of obesity and MetS, particularly under high-fat diet. Therefore, we took advantage of a transgenic mouse model previously developed in our group with expression of a constitutively active mutant of SGK1 to study the influence of the kinase in hepatocyte glucose production and to evaluate the expression of molecular markers of gluconeogenesis and glucose transport in wild type and Tg.sgk1 mouse liver before and after fasting.

RESUMEN

La importancia de la quinasa regulada por suero y glucocorticoides (SGK1) en la regulación del metabolismo energético se ha hecho evidente en los últimos años. Dicha serina/treonina-proteína quinasa forma parte de la ruta de señalización de insulina y es un objetivo transcripcional de los glucocorticoides. SGK1 parece jugar un papel importante en la regulación de la sensibilidad a la insulina, así como en la absorción y el metabolismo de la glucosa, y en el riñón promueve la reabsorción de Na^+, controlando así la presión arterial. El exceso de actividad de SGK1 se ha propuesto como un factor de riesgo para el desarrollo de obesidad y Síndrome Metabólico (MetS). Estudios previos desarrollados en nuestro laboratorio nos lleva a hipotetizar que la actividad de SGK1 incrementa la producción de glucosa mediante la activación de la gluconeogénesis, lo cual contribuye al desarrollo de obesidad y Síndrome Metabólico, particularmente bajo una dieta alta en grasa. Por lo tanto, aprovechamos el modelo murino previamente desarrollado en nuestro grupo con expresión de un mutante constitutivo de SGK1 para estudiar la influencia de esta quinasa en la producción de glucosa por hepatocitos y para evaluar la expresión de marcadores moleculares de gluconeogénesis y de transporte de glucosa en hígado de ratones *wild-type* y Tg.sgk1 antes y después de una situación de ayuno.

INTRODUCTION

Glucocorticoid hormones play a fundamental role in the control of embryonic development, cell differentiation, energy homeostasis, immune responses and the ability of animals to cope with different types of stressful situations. These steroids exert their regulatory effects through the glucocorticoid and mineralocorticoid receptors (GR and MR, respectively), intracellular receptors which act as potent transcriptional activators, or inhibitors of genes that possess glucocorticoid response elements (Webster, Goya et al. 1993). Serum- and glucocorticoid-induced kinases (SGKs) are transcriptional targets of steroid hormones including glucocorticoids and aldosterone. They belong to the AGC family and subfamily of serine/threonine protein kinases. Aside of all the well-known members of the AGC family as AKT, PDK1, S6K, PKC, and RSK, SGK kinases share a great sequence homology with the AKT family. It consists of three distinct but highly homologous isoforms (SGK1, SGK2, and SGK3) that are generated from three distinct genes localized on different chromosomes (Di Cristofano 2017). SGK1was originally cloned as an immediate/early gene transcriptionally stimulated by serum and glucocorticoids in rat mammary tumor cells (Webster, Goya et al. 1993). The human ortholog was then discovered as a cell volume-regulated gene upregulated by cell shrinkage (Waldegger, Barth et al. 1997). The gene encoding human SGK1 has been localized to chromosome 6q23, and it is expressed in nearly all tissues tested. However, transcript levels vary significantly among different cell types of any given tissues in the organism, including varying expression patterns during embryonic development. Subcellular localization of SGK1 is also complex and includes cytosolic, nuclear and membrane-associated fractions, with patterns that depend on the functional state of the cell (Lang, Bohmer et al. 2006).

Compared to most other protein kinases, a distinguishing feature of SGK is the stimulus-dependent regulation of its transcription, which includes enhancement by glucose, growth factors, osmotic stress and different steroid hormones (glucocorticoids, mineralocorticoids, estrogens and androgens).

Once synthesized SGK1 requires to be activated by the phosphatidylinositol-3-kinase (PI3K) pathway (Figure 1). This is accomplished through a signaling cascade involving the phosphoinositide-dependent kinases mTORC2 and PDK1. Therefore, SGK1 can be activated through the PI3K pathway by insulin, insulin-like growth factor (IGF-I), hepatic growth factor (HGF), and follicle stimulating hormone (FSH). SGK1 can also be activated by bone marrow kinase/extracellular signal-regulated kinase 5 (BK/ERK5), by p38(alpha), or by an increase of cytosolic Ca2+ activity (Lang, Bohmer et al. 2006). Maximal stimulation of SGK1 activity requires a first, mTORC2-dependent phosphorylation at Thr256 within the activation loop. This is followed by a PDK1-dependent phosphorylation at Ser422 in the hydrophobic motif (HM) at its COOH terminus (Garcia-Martinez and Alessi 2008, Yan, Mieulet et al. 2008).
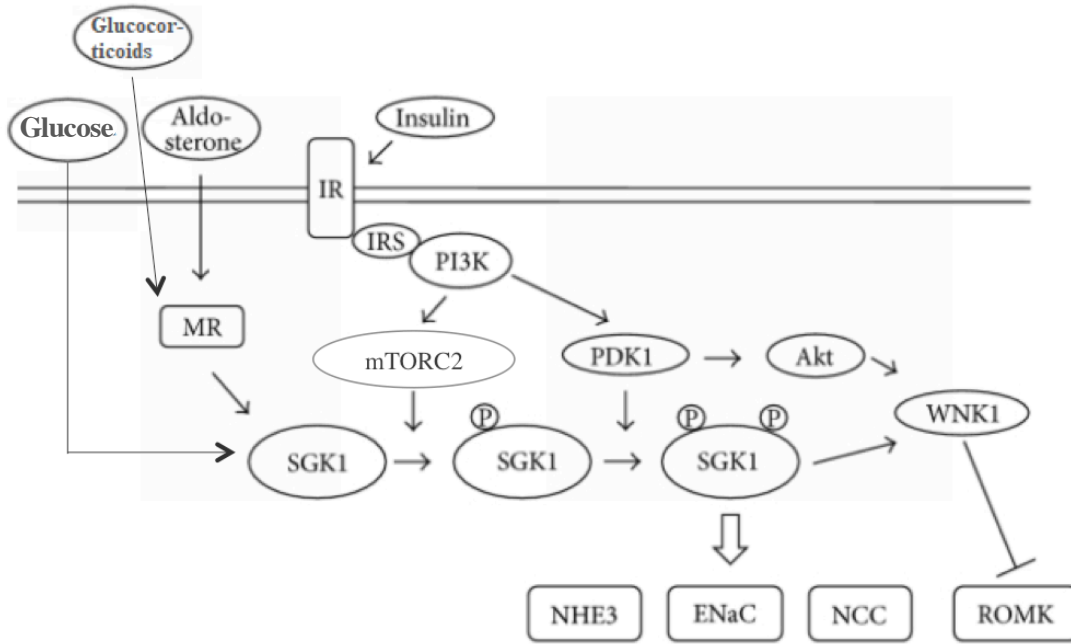
Figure 1. SGK1-mediated signaling pathway. Where aldosterone and glucocorticoids stimulate SGK1 via glucocorticoid receptor (GR), mineralocorticoid receptor (MR), glucose stimulates directly SGK1 and insulin stimulates it via IRS/PI3K pathway. SGK1 is phosphorylated twofold by PDK1 and mTORC2 [modified from (Satoh, Nakamura et al. 2015)].

Cellular signaling pathways controlled by SGK1.

There is evidence of SGK being an important focal point of intracellular cross-talk through which cell surface receptor, nuclear receptor, and cellular stress pathways converge to control many cellular processes, including cell proliferation, osmoregulation, and cell survival or apoptotic responses. SGK transcript levels can also be regulated in a tissue specific manner by osmotic changes, cytokines, TGF- β, ischemic injury of the brain, changes in cell volume, chronic viral hepatitis, aldosterone, DNA damaging agents, hypotonic conditions, heat shock, oxidative stress and UV irradiation, in addition to glucocorticoids, p53, FSH, and hyperosmotic stress (Firestone, Giampaolo et al. 2003).

SGK1 has been related to many cellular functions, phosphorylating the same proteins both *in vivo* and when overexpressed in cells. For instance, it mediates cell survival by preventing translocation of the transcription factor FOXO3a (Forkhead box O3a). This makes SGK1 a critical link between

growth and regulation of gene expression events that are very important for biological responses like cell survival and cell cycle reentry (Brunet, Park et al. 2001).

SGK1 has also been implicated in the control of membrane trafficking of a number of ion channels such as ENaC (epithelial sodium channel) (Arteaga, Alvarez de la Rosa et al. 2007) and several transporters including glucose facilitators (GLUT) (Lang, Bohmer et al. 2006, Mason, Cockfield et al. 2020). The most accepted mechanism by which SGK1 regulates membrane protein trafficking is indirectly by firstly phosphorylating and inactivating Nedd4-2, a ubiquitin ligase. This decreases the ability of Nedd4-2 to ubiquitinate ion channels or transporters; therefore, SGK1 will increase the amount of protein within the cell membrane (Lang, Bohmer et al. 2006).

Most importantly for this work, SGK1 modulates insulin signaling by phosphorylation of GSK3 (glycogen synthase kinase-3) (Murray, Campbell et al. 2004). GSK3 is a constitutively active and ubiquitously expressed serine/threonine kinase, and a very well stablished downstream component of the PI3K signaling pathway (Voskas, Ling et al. 2010). Since GSK3 is known to be a physiological substrate of PKB, Kobayashi and Cohen suggested the possibility of SGK1 phosphorylating directly or indirectly GSK-3β and then demonstrated it experimentally showing that SGK1 inactivates GSK3 by phosphorylation of Ser9 (Kobayashi and Cohen 1999). In further studies, it has also been reported that GSK-3β translocates from the cytoplasm to the mitochondrion after being phosphorylated in its Ser9 and being implicated in the mediation of mitochondrial functions. Mitochondrion is the sub-organelle in charge of the ATP synthesis, providing energy to the cells, carrying out the respiratory chain. Pyruvate dehydrogenase (PDH) converts pyruvate to acetyl CoA in the mitochondria and plays a key role in TCA cycle (tricarboxylic acid cycle), and glycolytic pathway. Since PDH has been demonstrated to be substrate for the

TPKI/GSK3β pathway, the activation of the GSK3β phosphorylates and suppress PDH, altering glucose metabolism in this way (Yang, Chen et al. 2017). Altogether, these pieces of information lead to the possible conclusion of SGK1 affecting the regulation of glucose metabolism via GSK3β.

SGK1 involvement in pathological processes.

SGK1 is implicated in a vast number of pathological processes within the organism. In regard of tumor growth, downregulation of SGK1 was found in prostate carcinoma (Rauhala, Porkka et al. 2005), ovarian tumors (Chu, Rushdi et al. 2002), and hepatocellular carcinoma (Chung, Sung et al. 2002). In addition, the inhibition of SGK1 expression by silencing RNA increased the toxicity of chemotherapeutic drugs in intestinal epithelial tumor cells. On the other hand, SGK1 expression mediates the glucocorticoid-induced resistance to chemotherapy of breast cancer (Lang, Bohmer et al. 2006).

SGKs have also been related to neuronal diseases due to the capacity to regulate AMPA and kainate glutamate receptors and upregulate glutamate transporters. As a consequence, variations of SGK expression could not only affect glutamate function but also, its clearance from the synaptic cleft (Lang, Bohmer et al. 2006). In addition, SGK1 could contribute to the glucocorticoid effects during cerebral injury including stroke, seizure, or hypo-glycaemia (Lang, Bohmer et al. 2006). It influences further carriers relevant for neuronal function, such as the creatine transporter (CreaT) which could lead to mental retardation, or the inositol transporter SMIT, which participates in neuronal cell volume regulation. SGK1 participates in the signaling of several neuropsychiatric disorders, such as schizophrenia, depression and Alzheimer's disease (Lang, Strutz-Seebohm et al. 2010). Recent studies with a neuronal-specific isoform of SGK1, SGK1.1, show that its activation can be a possible protection factor in the brain against

11

permanent neuronal damage associated to epilepsy (Armas-Capote, Maglio et al. 2020).

There is strong evidence that MR-mediated SGK1 expression increases blood pressure due to upregulation of renal salt reabsorption (Satoh, Nakamura et al. 2015). SGK1 also regulates kidney growth and glomerular permeability, induces hypokalemia (Vallon, Huang et al. 2005), and mediates the effect of mineralocorticoids in salt appetite (Lang, Bohmer et al. 2006). This kinase also contributes to dysregulation of cellular Na^+ and water transport in diabetes mellitus, alters sodium flux leading to arrhythmia, and it is involved in cardiomyopathy, cardiac hypertrophy and progression to heart failure (Lou, Zhang et al. 2016).

SGK1 Implications in Metabolism.

In addition to being downstream of the insulin receptor, SGK1 is a transcriptional target of glucocorticoids and mineralocorticoids, two types of hormone crucially important to cope with environmental or endogenous stress and, in the case of glucocorticoids, important regulators of energy homeostasis. This suggests that SGK1 could play an important role in modulating glucose metabolism and provide a convergence point between cardiovascular and metabolic regulation. SGK1 could potentially participate in conditions characterized by disorders in blood pressure regulation and energy metabolism, such as the Metabolic Syndrome (MetS). It has been found that two SGK1 gene variants, in intron 6 (I6CC), and exon 8 (E8CC or E8CT) correlate with higher diastolic and systolic pressure respectively, are associated with increased blood pressure progression rate, higher prevalence of hypertension, and a stronger correlation between fasting plasma insulin concentration and diastolic blood pressure (von Wowern, Berglund et al. 2005). This study supported the important role of SGK1 in blood pressure regulation in humans, but also provided one of the first

suggestions that it is also involved in the regulation of glucose handling and metabolism. Consistent with this notion, studies using SGK1 inhibitor EMD638683 have lowered blood pressure in mice fed with a high-fructose and high-salt diet (Ackermann, Boini et al. 2011), and in db/db mice, a model of type 2 diabetes mellitus, inhibition of SGK1 presented a beneficial effect in obesity and hyperglycemia (Li, Hao et al. 2016).

SGK1 has been described as a stimulator of the Na^+-coupled glucose transporter SGLT1, which accelerates intestinal glucose absorption leading to excessive insulin release, fat deposition and lower plasma glucose concentrations. Inhibition of SGLT1 neutralizes obesity (Lang, Artunc et al. 2009). SGK1 also stimulates the expression of glucose transporter GLUT1 which promote glucose uptake from plasma to the tissues (Lang, Bohmer et al. 2006, Mason, Cockfield et al. 2020). It has long been known that excess salt intake impairs cellular glucose uptake, leading to glucose intolerance. Stimulation of MR with the mineralocorticoid deoxycorticosterone acetate (DOCA) restores glucose tolerance and insulin sensitivity in wild-type mice (WT) on a high-salt diet, but not in SGK1 knockout mice (Lang, Bohmer et al. 2006). Therefore, SGK1 does not only combine the mineralocorticoids and insulin effects in renal tubular Na^+ transport (Alvarez de la Rosa and Canessa 2003), but it appears to play a critical role in glucose transport as well.

SGK isoforms have also been related to the stimulation of glucose transport via its role phosphorylating GSK3 (Lang, Bohmer et al. 2006). Activation of the aldosterone/MR pathway might be critically involved in the development of obesity-induced salt-sensitivity hypertension through sodium retention in the body (Fujita 2008). This hypothesis is supported by previous studies which demonstrated that aldosterone increases sodium reabsorption by activation of ENaC in the distal tubule, possibly through SGK1 (Fujita 2008).

Taking together all pieces of evidence of SGK1 affecting blood pressure, plasma insulin concentration, obesity, glucose uptake and transport, led to study the possible correlation between SGK1 and the pathophysiology of metabolic syndrome (MetS) (Lang, Bohmer et al. 2006). MetS is a pathologic condition characterized by the co-occurrence of several cardiovascular risk factors, including abdominal obesity, insulin resistance, hyperlipidemia, and hypertension (Huang 2009, Saklayen 2018). A recent study from our laboratory examined the effects of excess SGK1 activity in the different MetS conditions taking advantage of a mouse model previously developed in our group. This model (Tg.sgk1) was created by pronuclear injection of a bacterial artificial chromosome (BAC) containing the whole mouse SGK1 gene modified by insertion of 3xHA epitopes added to the C-terminus. The BAC contains the promoter, enhancers, and other regulatory elements of the SGK1 gene assuring this model would keep the same transcriptional control and would process as the SGK1 endogenous alleles. Tg.sgk1 mice show increased fasting plasma glucose levels, suggesting a dysregulation of glucose handling (Sierra-Ramos, Velazquez-Garcia et al. 2020). Feeding this animal with a high-fat diet, in six weeks it developed all possible metabolic factors in MetS, such as hypertension, dyslipidemia, insulin resistance, glucose intolerance, body weight gain, visceral adiposity NAFL non-alcoholic fatty liver (Sierra-Ramos, Velazquez-Garcia et al. 2020). All these metabolic conditions increase the risk to develop cardiovascular disease, diabetes mellitus type 2, chronic kidney disease, cancer, and nonalcoholic steatohepatitis (Kaur 2014). Our study supports a role for SGK1 as a risk factor to develop MetS and points to its interest as a possible therapeutic target in metabolic syndrome. Work from a different group found that liver-specific SGK1 knockout decreases insulin sensitivity (Liu, Yu et al. 2014). Taken together, these data suggest that correct SGK1 signaling is an important factor in regulating energy homeostasis and glucose handling.

Together, all these data led our research group to a new study which remains unpublished, where we tested the effects of metformin as a proof-of-concept to use Tg.sgk1 mice as a in vivo platform to perform pre-clinical testing of new drugs. Metformin is an oral hypoglycemic agent which is most widely used as first-line therapy for type 2 diabetes. It improves glycemia by suppressing hepatic glucose production and increasing glucose uptake in muscle, reducing cardiovascular events (Figure 2). The mechanism by which metformin lowers glucose levels in the organisms has been proved to be via suppression of gluconeogenesis in the liver targeting the activated protein kinase (AMPK), an energy sensor activated under metabolic stress. This kinase inhibits glucose liver production, improves insulin sensitivity and glucose uptake by muscle, and induces fatty acid oxidation (Saisho 2015).
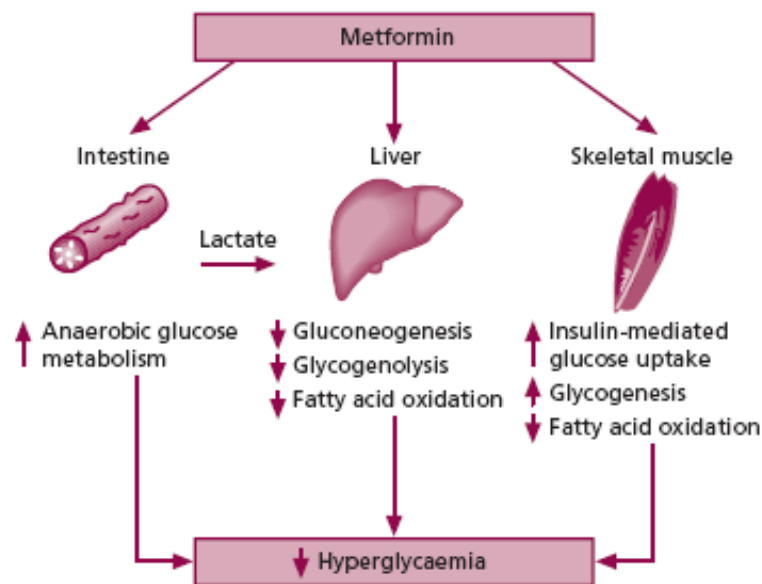
Adapted with permission from Bailey CJ, Feher MD, Therapies for Diabetes, Sherborne Gibbs, Birmingham UK, 2004

Figure 2. Metformin targeting-organs and metabolic results leading to the decrease of glucose levels in plasma.

The results obtained after treating WT and Tg.sgk1 mice with metformin, while still being fed with high-fat diet supports the conclusion that Tg.sgk1 show increased sensitivity to metformin. Treated mice reduced body weight without affecting food intake and improved glucose homeostasis (S.

Velázquez-García and D. Alvarez de la Rosa, unpublished). Fasting glucose levels were measured at the beginning of the HFD treatment and during the metformin treatment, and Tg.sgk1 metformin-treated mice showed a significant decrease in blood glucose levels since the first 3 weeks of the study, unlike WT metformin-treated mice which started to see effect after 5 weeks of treatment (Figure 3A and B). Glucose tolerance tests (GTT) were performed after 5 weeks of metformin treatment, and in Tg.sgk1 metformin-treated mice, glucose levels in blood do not only not reach such high levels as without the metformin treatment, but the rate at which glucose is taken from the blood is remarkably faster (Figure 3C). Insulin tolerance test (ITT) were performed after 3 weeks of treatment and Tg.sgk1 metformin-treated mice already presented substantial improvement compared to both non-treated tg. sgk1 mice and WT mice (Figure 3D) (S. Velázquez-García and D. Alvarez de la Rosa, unpublished).
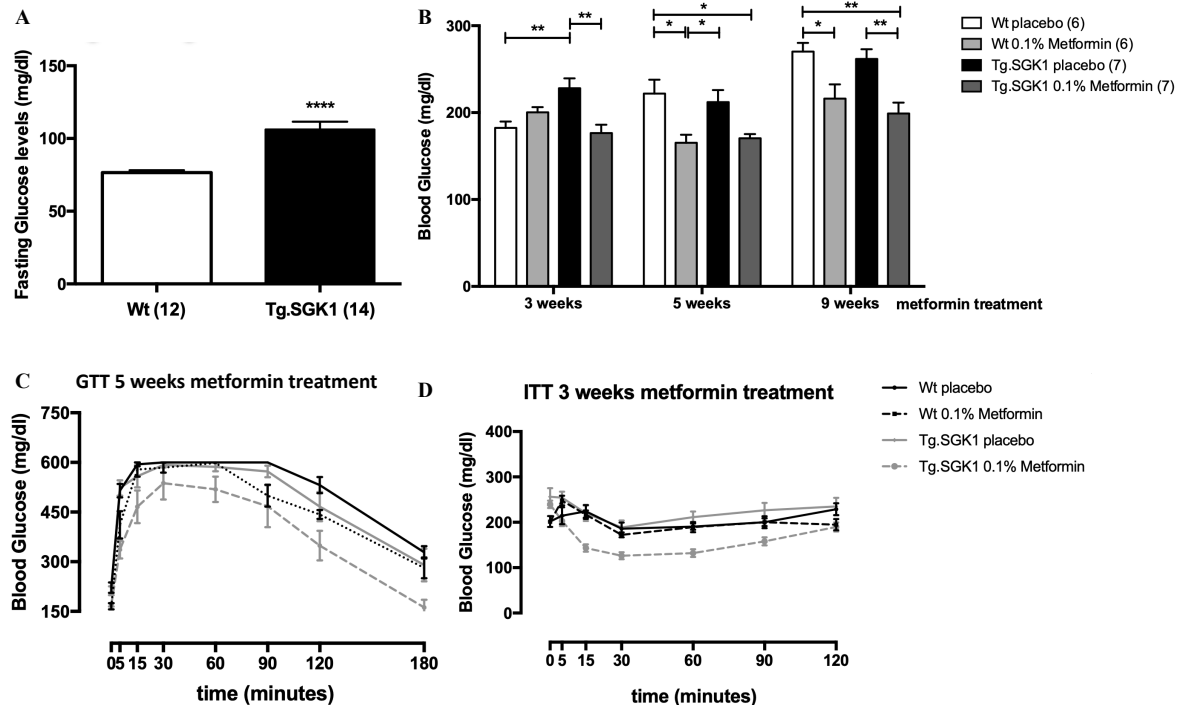

Figure 3. Unpublished metformin study from our group. (A) Fasting glucose levels before HFD treatment. (B) Fasting blood glucose level evolution during metformin treatment. (C) Glucose Tolerance Test showing blood glucose levels after 5 weeks in metformin

treatment. (D) Insulin Tolerance Test showing blood glucose levels after 3 weeks in metformin treatment (S. Velázquez-García and D. Alvarez de la Rosa, unpublished).

Hepatic glucose production accounts for nearly 90% of endogenous glucose production, and it is crucial for systemic glucose homeostasis. During fasting, glucose levels are prevented from dropping too low through two hepatic processes, glycogenolysis, the degradation of glycogen, and gluconeogenesis, the generation of glucose from non-carbohydrate carbon substrates including pyruvate and lactate (Figure 4) (Petersen, Vatner et al. 2017). This situation contrasts with the fed state, where glucose enters in the liver via GLUT2, it is phosphorylated in hepatocytes to create glucose 6-phosphatase (G6P) leading to a reduction in intracellular glucose concentration. G6P stays within hepatocytes in fed state to act as a precursor for glycogen synthesis, or to be metabolized through glycolysis to form pyruvate. Pyruvate is completely oxidized to generate ATP through the TCA cycle and oxidative phosphorylation, or pyruvate could also be used to synthesize fatty acids through lipogenesis (Rui 2014).
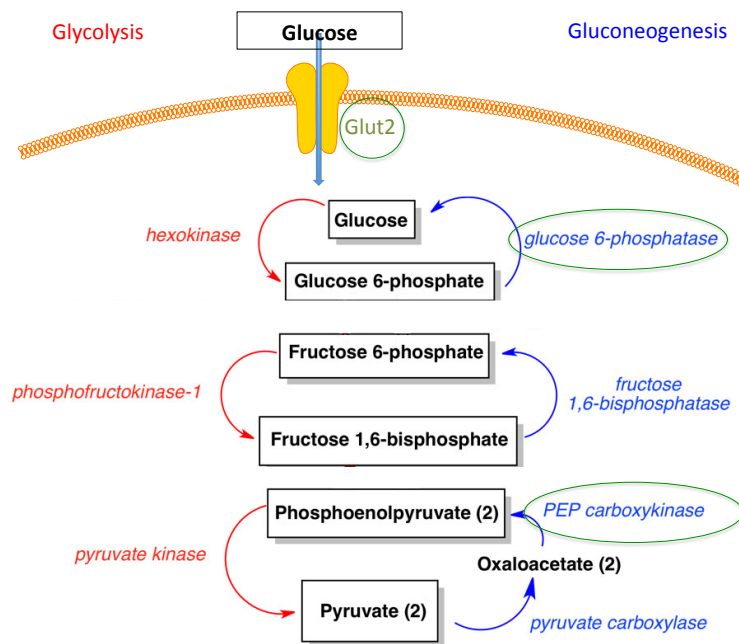

Figure 4. Glycolysis and gluconeogenesis pathway.

In an unpublished experiment performed in our laboratory, mice were subject to a pyruvate tolerance test (PTT) after 9 weeks treatment with metformin. In PTT, pyruvate is injected, and it elicits a glycemic excursion which reflects hepatic gluconeogenesis. The experiment demonstrated that blood glucose levels do not reach as high in animals treated with metformin as they do when they are not treated, as expected (Figure 5). More importantly, in untreated mice, Tg.sgk1 showed a higher glycemic excursion, suggesting increased gluconeogenesis under fed conditions (Figure 5). Treating Tg.sgk1 mice with metformin also improved hypertension induced by high-fat diet and regulated gluconeogenesis markers (GLUT2, G6PC and PCK1) at the mRNA level (S. Velázquez-García and D. Alvarez de la Rosa, unpublished).
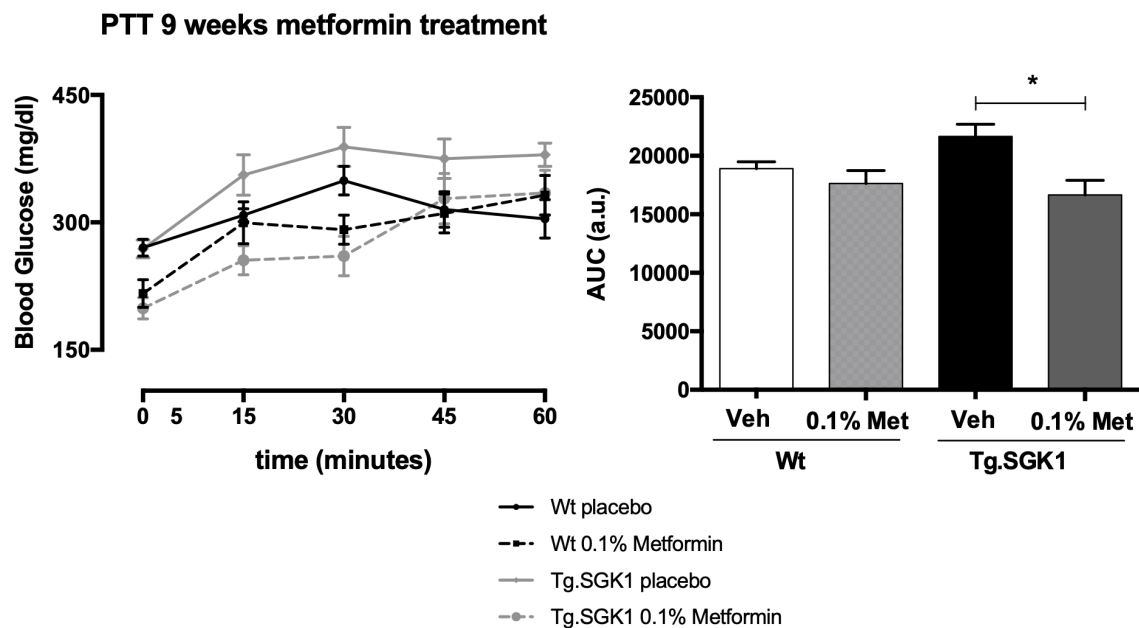
Figure 5. Unpublished metformin study from our group. Pyruvate Tolerance Test (PTT) showing blood glucose levels after 9 weeks in metformin treatment A) Glycemia time-course after the intra-peritoneal injection of pyruvate. B) Area under the curve (AUC) derived from the PTT curves, used as an index of the glycemia excursion. One-way ANOVA followed by Bonferroni´s test. *, $p < 0.05$ (S. Velázquez-García and D. Alvarez de la Rosa, unpublished).

These results and the fact that Tg.sgk1 mice show increased fasting glycemia, indicate that SGK1 may increase glucose production by abnormally up-regulating gluconeogenesis.

HYPOTHESIS AND OBJECTIVES

Hypothesis:

SGK1 activity increases glucose production by activating gluconeogenesis, which in turn contributes to the development of obesity and Metabolic Syndrome.

General Objective:

To study whether hepatocytes from transgenic mice with increased SGK1 activity produce excess glucose, and how.

Specific Aims:

1. To compare glucose production in wild type and Tg.sgk1 mouse hepatocytes.
2. To evaluate the expression of molecular markers of gluconeogenesis and glucose transport in wild type and Tg.sgk1 mouse hepatocytes.
3. To test whether gluconeogenesis is activated in mouse during fasting, and compare wild type and Tg.sgk1 mice.

Material and Methods

Hepatocyte Isolation

Primary mouse hepatocytes are an important tool in the biomedical research field for the assessment of hepatocyte function. Hepatocytes are involved in many biological processes including protein synthesis, sugar metabolism, detoxification, as well as synthesis and secretion of cholesterol, bile acids, and phospholipids (Severgnini, Sherman et al. 2012). Our first technique approximation for hepatocyte isolation is based on the two-step collagenase liver perfusion, which requires firstly, the removal of calcium ions from epithelial cells by using EGTA 100mM, for then start the enzymatic digestion with collagenase 1mg/ml (Li, Ralphs et al. 2010).

Each mouse was anesthetized using 20% Dolethal via intraperitoneal injection. When they were 100% unconscious the abdominal area was cleaned with 70% ethanol to reduce the possibility of infection before performing an "U"-shaped incision through the skin of the lower abdomen to the lateral aspects of the rib cage. Search for the portal vein by moving intestines and organs as needed, preferably to the right. Using blunt forceps we gently made our way under the portal vein, removing any adipose tissue and used it later as support to insert the cannula. We secured the cannula using a standard dressing forceps and allowed perfusion medium 1 (Table 1) to enter the liver. Once the liver started to change to a whitish color (Figure 6), we cut the inferior vena cava to allow the liver to clear of blood. We finished perfusion of mediums 2 and 3 (Table 1) for approximately 10-15 minutes at a rate of 5 ml/min. Once the collagenase solution was completely perfused into the liver, the organ turned very delicate and slippery for dissection, and thus a spoon is usually necessary to carry it out.
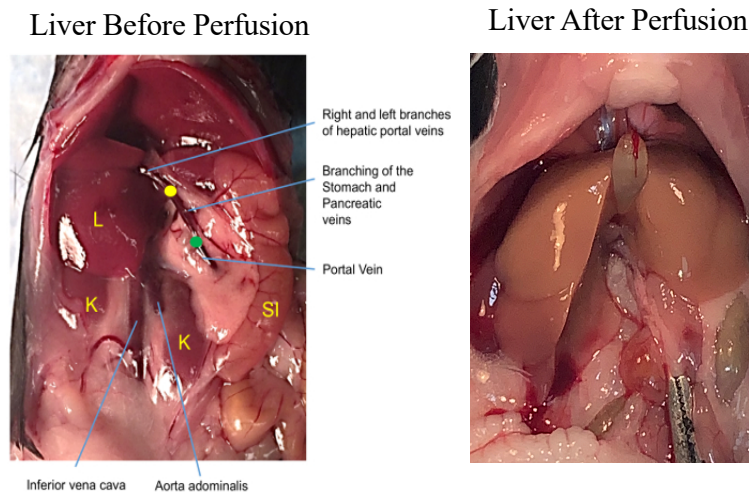
Liver Before Perfusion

Liver After Perfusion

Figure 6. Liver appearance before perfusion and portal vein where cannulation and perfusion took place (on the left). Liver appearance after perfusion (on the right).

Hepatocyte Culture.

Prepare a 100 mm Petri dish with 5ml of perfusion medium 1 (Table 1) at the end of the perfusion to place the liver and take it to the culture hood. Start dissociating the liver lobes using two pair of forceps, and if possible, remove its connective tissue layer. Shake gently the dissociated liver to release the residual parenchymal cells into the medium and add another 15 ml cold Dulbecco´s modified Eagle's medium (DMEM) to the Petri dish to get the rest of the cells. Filter the crude hepatocyte preparation through a 100 μm gauze mesh filter and transfer the resulting cell suspension into two 50 ml sterile tubes. Hepatocytes are found in the pellet after centrifuging at 100 x g for 3 minutes at 4ºC (Figure 7). Discard the supernatant and wash the cells using the liver wash media (DMEM) three to four times. Once the supernatant remains clear, replace the medium with Hepatocyte Maintenance Medium (HMM, Lonza) supplemented with dexamethasone, insulin and GA-100 as required by manufacturer's instructions (Lonza), count the cells using hemocytometer and trypan blue, and plate cells for overnight incubator at 37ºC. Plates were coated with 1ml of Bovine Collagen Coating Solution 24 hours prior to plating the cells, left at room temperature overnight and washed with PBS prior to plating the cells (Figure 8).
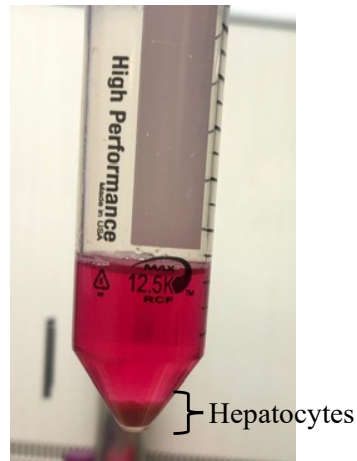
Figure 7. Hepatocyte pellet after first wash with DMEM.

SOLUTION	CHEMICAL COMPOSITION
HBSS (1x)	Calcium Chloride (anhydrous) 1.25 mM, Magnessium Chloride 0.81 mM Magnesium Sulfate (anhydrous), Potassium Chloride 5.36 mM, Potassium Phosphate Monobasic (anhydrous) 0.44 mM, Sodium Chloride 136.8 mM,, Sodium Phosphate Dibasic (anhydrous), 0.33 mM, D-Glucose 5.5 mM, 0.35g/L Sodium bicarbonate
Solution 1	**HBSS(1x) + HEPES** HEPES 1.1915g/500 ml
Solution 2	**HBSS(1x) + EGTA (1mM)** 2.5 ml EGTA 100mM to 250 ml HBSS (1x). 0.95g of EGTA in 25 ml H2Oq (add NaOH to completely dissolution)
Solution 3	**Solution1 + Collagenase (1mg/ml)** (Sigma Aldrich #C9891)
Bovine Collagen Coating Solution	(Sigma Aldrich #125-50 SAFC)
Dulbecco's Modified Eagle's Medium (DMEM)	(Sigma Aldrich #D5796). Supplemented with 1g/L glucose, 0.584g/L L-glutamine 3.7 g/L sodium bicarbonate
Hepatocyte Maintenance Medium (HMM)	(Lonza, #CC-3199). Supplemented with hydrocortisone, insulin and GA-100 cocktail (Lonza #CC-4182)

Starvation Medium	DMEM: glucose-free (Sigma Aldrich #5030); 0.584g/L glutamine and supplemented with 1mM pyruvate.
Induction Medium	Starvation Medium + 500μM 8CPT + 100μM dexamethasone.
Lysis Buffer Solution	**RIPA 1%** - Tris HCL 50mM (ph 7.4)+ NP-40 1% + Na deoxycholate 0.5% (w/v) + SDS 0.1% + NaCl 150 mM + EDTA 2mM. Supplemented with PhosphoSTOP 1x (Sigma Aldrich #PHOSS-RO) and Complete Inhibitor Cocktail 1x Roche #04693132001
TBST-T	Tris- HCl 40 nM, NaCl 0,8%, Tween-20 0,05%

Table 1. Solution summary.

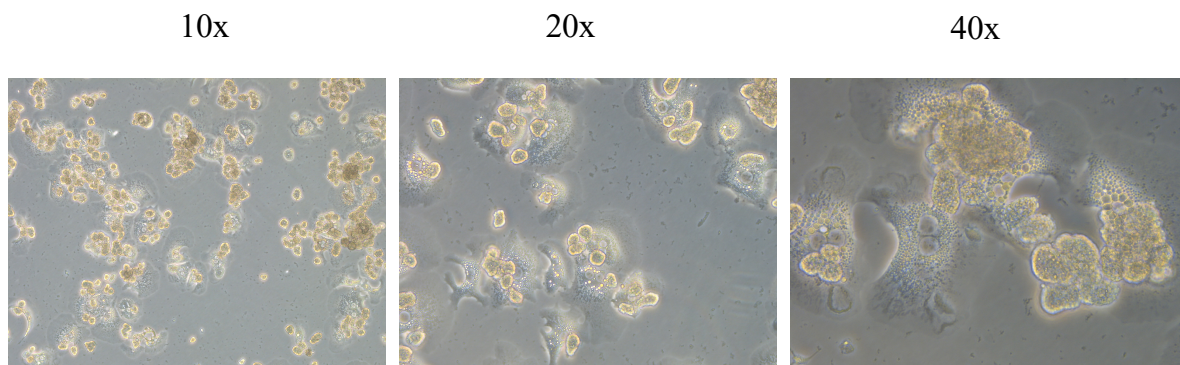| 10x	20x	40x

Figure 8. Wild type hepatocytes after 22 hours plated.

Treatments for Glucose Production.

After incubation for 24h with HMM (table 1), hepatocytes were switched to incubation with a medium without glucose. To do that we used the following media:

Starvation Medium: Primary hepatocytes were treated 24 hours after being cultured with 2ml/well of Dulbecco's Modified Eagle's Medium (DMEM),

prepared without glucose, containing glutamine and supplemented with 1mM pyruvate (table 1) (Calabuig-Navarro, Yamauchi et al. 2015, Goldstein, Baek et al. 2017).

After this time, hepatocytes were incubated either with or without an Induction Media for 24h:

Induction Medium: 24 hours after starvation medium, hepatocytes were treated with 2ml/well of starvation medium + 500 µM 8-CPT + 100µM dexamethasone (table 1). The purpose of this treatment is to induce glucose production in hepatocytes and compare it to the parallel line that remains in starvation medium (Calabuig-Navarro, Yamauchi et al. 2015).
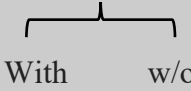
Monday	Tuesday	Wednesday	Thursday	Friday
WT. & Tg. liver extraction	Starvation Medium Replacement	Induction Medium Replacement With w/o	-Glucose measurement -RNA extraction -Protein Extraction	…

Table 2: Week organization of cell treatments replacement followed in this study.

Glucose Production Assay.

After 24 hours of induction medium, 1ml of the hepatocyte supernatant was collected and stored at -80ºC. Glucose levels were determined using the High Sensitivity Glucose Assay Kit (Sigma–Aldrich #MAK181) following the manufacturer's instructions. Fluorescence intensity was measured using Perkin Elmer VICTOR multilabel plate reader using the manufacturer´s software.

Protein Extraction and Quantification.

After collecting the supernatant for measurement of glucose production, cells were washed with PBS and treated with Lysis Buffer Solution (Table 1), Radioimmunoprecipitation assay (RIPA 1%), which is a rapid, efficient cell lysis and solubilization of proteins from cultured mammalian cells. RIPA was supplemented with PhosphoSTOP 1x and Complete Inhibitor Cocktail 1x from Roche. The sample was collected in autoclaved Eppendorfs for further lysis, centrifugation and protein quantification. Protein concentration in the supernatant was estimated using the colorimetric method of Bicinchoninic Acid (BCA, Sigma Aldrich).

Liver Tissue Extraction.

Liver extraction was performed using animals fed normal chow of after 24h fasting (WT, n=6; Tg.sgk1, n=8). Animals were weighted before and after fasting. Following the sacrifice of the animal by cervical dislocation, the abdomen was cleaned and a U-shape incision in the abdominal cavity was performed to extract the whole liver. The organ was divided and weighted using a precision balance and a piece of aluminum. Each piece was placed in different Eppendorf tube and frozen in liquid N_2 for further RNA and protein extraction and quantification.

Western Blot.

Protein extraction and quantification from liver tissue was as described for cultured hepatocytes. 40 μl of protein were loaded into TGX Stain-Free polyacrylamide electrophoresis gels (Biorad, 4-15% concentration gradient). The electrophoresis was performed in a mini-PROTEAN apparatus (Biorad) at a constant voltage of 180 volts for 60 minutes. Then proteins were transferred to a 0.2 μm polyvinylidene difluoride (PVDF) membrane using the Trans-Blot Turbo Transfer system (Biorad). Membranes were then blocked with 5% Milk in TBS-T (Table 1) for 1h and incubated at 4ºC with

in 5% non-fat dry milk, 1x TBS. Afterwards, membranes were washed 3-5 times with TBS-T and incubated in 0.5% non-fat dry milk in diluted secondary antibody (anti-mouse or anti-rabbit antibodies conjugated to horseradish peroxidase; Jackson, 1:10000). Finally, to reveal signals, each membrane was incubated in a 1:1 ratio of Clarity Western ECL Peroxide Solution and Luminol/Enhancer Solution (Biorad) for 5 min. The chemiluminescent signal was then detected using a system equipped with a CCD camera (ImageQuant LAS500, GE Healthcare).

Antibody	Supplier	Protein Size	Dilution
Anti-G-6-Pase	(ab83690)Abcam	40kDa.	(2 ug/ml)
Glut2	(sc-518022) Santa Cruz Antibodies	60-62 kDa	1:500
PEPCK1	(sc-377027) Santa Cruz Antibodies	67 kDa	1:500

Table 3: Primary antibodies used in this study.

RNA Extraction.

The RNA was purified from whole liver following first the Tripure Isolation Reagent Protocol from Roche, and then, as it was purified from hepatocytes, using the commercial kit *NucleoSpin mini Kit RNA* (Macherey-Nagel). RNA for both sources was measured, and its quality was assured by spectrophotometry using the Nanodrop 1000 equipment (Themo Scientific).

Real-time quantitative polymerase chain reaction (qPCR).

The RNA samples (1 µg) were submitted to reverse transcription to its complementary DNA (cDNA) using the iScript cDNA Synthesis Kit (Bio-Rad) following the manufacturer's instructions. qPCR was performed using a CDX96 thermal cycler (Biorad). The detection method for DNA

amplification was the *iQ^{TM} SYBR Green® Supermix* kit (BioRad). The protocol followed for the amplification was: 95 ºC, 3 minutes; 40x (95°C, 10 minutes, Tm, 20 sec, 72 °C, 15 sec); denaturation temperature ramp (65 ºC, 5 min; temperature of 95 ºC to 0.5ºC). The threshold amplification cycle (Ct) value was used as measurement parameter of the expression of a gene, which is inversely proportional to the amount of specific template DNA. To determine the relative level of expression of the genes of interest in each group, a housekeeper, RPL13Awas used as reference (Table 4) (Radonic, Thulke et al. 2004, Rubie, Kempf et al. 2005).

GEN	AnnealingTemp. PCR		Sequence (5' to 3')
Glut1	62	Fw	TCACGGATGCCAATTACCGA
		Rv	TGCCAGCTGTCTGAAAAATGC
G6Pc	62	Fw	TGAGACCGGACCAGGAAGTC
		Rv	GCAAGGTAGATCCGGGACAG
PCK1	62	Fw	TGCGGATCATGACTCGGATG
		Rv	AGGCCCAGTTGTTGACCAAA
RPL13A	62	Fw	TATCTGCACTGCCAAGACTGAGTG
		Rv	CTGGTACTTCCACCCGACCTC

Table 4: Primers used in this study.

RESULTS AND DISCUSSION

Due to the unfortunate detention of all laboratory experiments and activities as a consequence of the COVID-19, the results I can report from this project are limited. The hepatocyte preparation had not been performed before in our laboratory and it is essential towards the understanding the role of SGK1 in liver metabolism and the participation of this process in the accelerated development of MetS. As it has been mentioned before, the hepatocyte isolation is an extremely challenging procedure not only due to the delicacy of these cells but also due to the low success ratio of this preparation (Orfan Biotech, personal communication). Therefore, most of my laboratory effort before the start of the emergency situation and lockdown was focused on setting up the hepatocyte primary culture model.

*Hepatocyte preparation: optimization of the perfusion procedure*

Firstly, I performed the hepatocyte isolation following the protocol described in the Material & Methods section, but instead of perfusing from the portal vein, I first learned to insert the cannula through the common bile duct. I found this procedure more complicated since it is a duct smaller in diameter, and the walls are more slippery than the portal vein's, which makes it easily breakable. If perfusion through the common bile duct would not work, we would then insert the cannula through the portal vein, since our first understanding of this protocol was that this first duct was the best via to perfuse the liver. Given the experience obtained in the first preparations, we switched to the portal vein access for routine perfusion. We also did not count with a perfusion pump to impulse the reagents through the cannula, so we improvised a perfusion system with three syringes, a three-way tap and perfusion tubing, one syringe for each solution. Therefore, we would ensure manually the perfusion rate of 5 ml/min for each solution. In addition, we used a heating blanket to keep the solutions warm while perfusing, at the

right temperature for liver enzymes digestion, since the syringe with the solution would spend around 15 to 20 minutes outside the warm bath.

Hepatocyte culture optimization and cell characterization

During the first attempts at establishing the primary hepatocyte culture model in our laboratory, we obtained very variable outcomes, with divergent cell yields, cell mortality and different shapes and morphological characteristics. We thus performed a detailed bibliographical search on the characteristics of mouse primary hepatocyte cultures. Cell morphology is characterized by its prototypical spherical shape which they maintain during the first hours of culture. During this first period hepatocytes can grow individually or in small clusters. After 24 hours, viable cells start to flatten and tend to grow closely together in groups. At the microscope, most of these flatten and spread hepatocytes appear to have two rounded nuclei of similar size, bile canaliculus-like structures, tight junctions and desmosomes between each other along their membranes. Autophagic vacuoles are also characteristically found in the cytoplasm together with mitochondria of different shapes and sizes (Klaunig, Goldblatt et al. 1982). According to this same article, after two hours of culture, almost 90% of the cells plated present areas of translucent gray space, which James E. Klaunig et al. believe it is the former site of glycogen lost during the extraction procedure.

In order to improve our methodology, we optimized several parts of the procedure. First, we proved experimentally while optimizing this protocol that hepatocytes plate better in collagen-coated plates washed with PBS prior to the procedure than in plates with no PBS wash (Figure 9).

10x	20x	40x
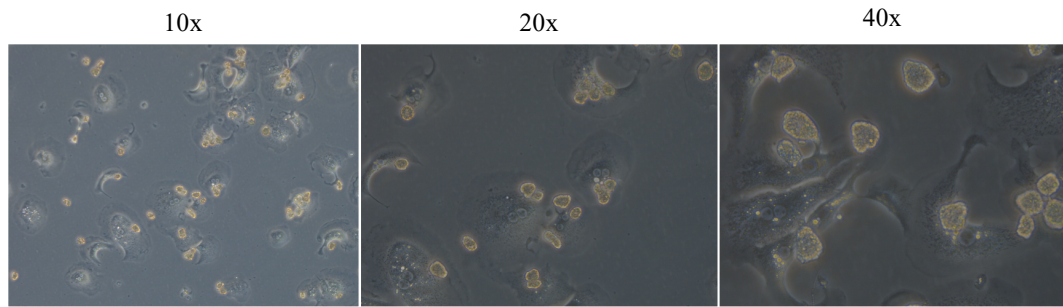
Tg. SGK1 hepatocytes 17h after HBM replacement with PBS wash

10x	20x	40x
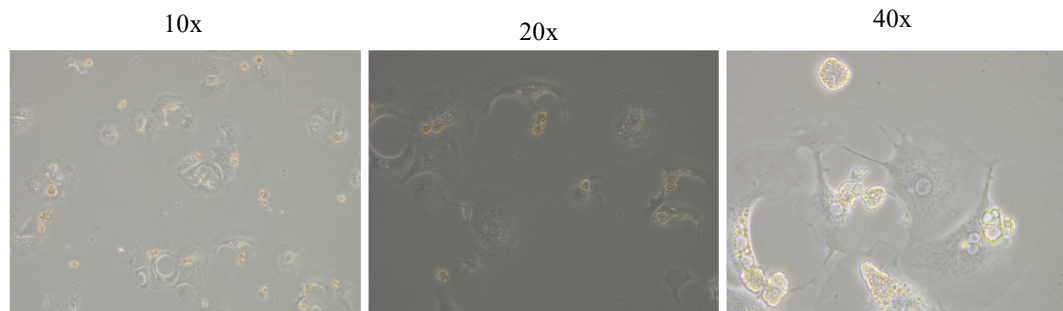
Tg. SGK1 hepatocytes 17h after HBM replacement NO PBS wash

Figure 9. Tg.sgk1 hepatocytes in plates with PBS wash (on top). Tg.sgk1 hepatocytes in plates with no-PBS wash (on the bottom).

In addition to the regular protocol, and after several attempts that yielded very few living cells, we decided to improve the viability of our cells by introducing a purificaton protocol based on centrifugation through Percoll, as described in *iron.med.ucla.edu*. We were able to locate an intermediate layer between the DMEM medium and the Percoll cushion where all our hepatocytes were located. According to *iron.med.ucla.edu,* this layer should contain all dead cells, while living cells should precipitate to the bottom after centrifugation. We observed the supposedly dead cells under the microscope and analyzed them with an automatic cell counter using the Trypan blue exclusion method, and found that this layer contained all our hepatocytes, with a mixture of living and dead ones. Suspecting a problem with the 100% Percoll solution, we then moved to different experimental strategy using different Percoll density layers (Figure 10) and creating a gradient in the tube with 6ml of our cell suspension in DMEM (Figure 10). After 20 minutes

centrifugation we again did not find the expected hepatocyte pellet, strengthening our assumption of being something wrong with our 100% Percoll solution.
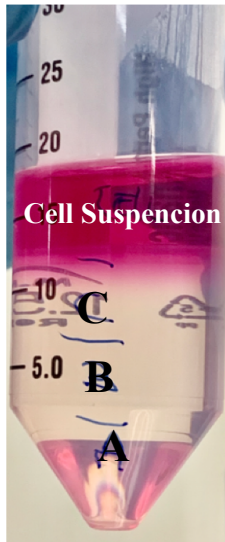
Percoll Density Layers.		
A	3ml of 1.12g/ml	100%
B	5ml of 1.08 g/ml	96.4%
C	5ml of 1.06 g/ml	94.6%

Figure 10. Percoll density layers in a 50ml Flacon Tube (on the left). Preparation of each Percoll density layer (on the right).

The next experiment tried further changes in the hepatocyte isolation protocol using the Percoll purification step. To improve hepatocyte disaggregation, we introduced the cannula through the portal vein and blocked the back flow and the loss of our perfusion solution through the common bile duct by knotting it very carefully with suture. We also knotted with suture the portal vein with the needle once we were in and ready to start perfusing. We divided the cells suspension after the first wash into two tubes. An aliquot of cells was treated with 40% percoll (aliquot 1) following *iron.med.ucla.edu* protocol, and the other was handled according to the original isolation protocol (aliquot 2). In aliquot 1 we obtained again the middle layer with mixed hepatocytes and no pellet. However, this time we decided to take the supernatant and the intermediate cell layer, centrifuged it and characterized it using the automatic cell counter and Trypan blue exclusion. The method reported good viability, and therefore we plated those cells. We plated hepatocytes from aliquot 2 as well, after observing no dead

hepatocytes in the supernatant after second wash, which led us to assume that the pellet contained all living hepatocytes. Unfortunately, checking these two groups of cells the next day, they were all in suspension floating in the medium, which means they did not survive to the procedure.

Some more culture attempts involved a few changes like adding a second gauze mesh strainer of 40μm in diameter and replacing the DMEM medium 2 to 3 hours after plating to HMM (Figure 11). However, our cells kept dying after one day of culture.
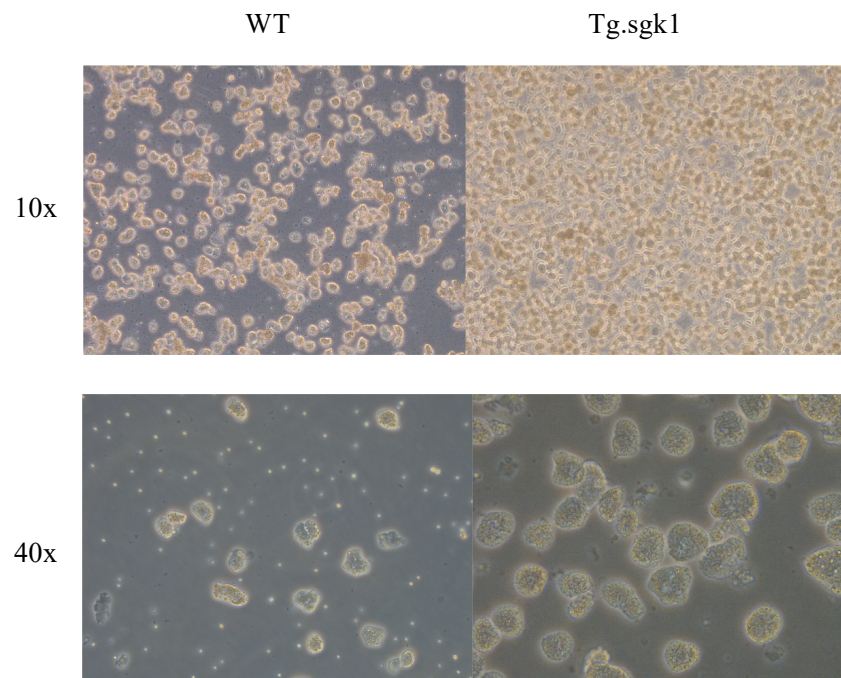
Figure 11. Wild Type and Tg.sgk1 hepatocytes . Plated in DMEM 4h post plating (on top). After the HMM replacement 4 h post culture.

After spending a week analyzing and researching what we could possibly had been doing wrong, we decided to meet with two scientists from *Orfan Biotech*, who are experts in the hepatocyte isolation procedure. Based on their advice, we introduced the following improvements: the syringe perfusion system was substituted by a constant perfusion pump to control and limit the pressure used during the procedure; all mediums were switched to commercially available ones (Gibco Life Technologies) (Table 5); we

included penicillin and streptomycin in all solutions and washed the perfusion tubing system with antibiotics to avoid any contamination; in addition, we included a disinfect step using iodopovidone to clean the mouse abdominal area prior to the incision; the needle to cannulate the portal vein was switched from a 23G to a 27G caliber to avoid excessive pressure while perfusing; liver and cell treatment was changed to avoid mechanical damage to the material; switch to use of plastic Pasteur pipettes to avoid possible damage from the glass pipettes; elimination of the second strainer in the filtering procedure; cells were kept inside the incubator while counting them with the hematocytometer or the automatic cell counter (Figure 12A); finally, we introduced a last wash with William's E Medium, avoiding any change in medium until after overnight incubation after plating.

We followed this improved protocol in our next attempt and we finally obtained cultured living hepatocytes around 20 to 40 hours after plated. However, the yield was not as high as we expected for the number of cells we started with, and the mortality was still high during the first 20 hours (Figure 12B, C and D).

Recommended Mediums from Gibco Life Technologies	
Liver Perfusion Medium	Supplemented with 10ml penicillin-streptomycin (100x). (Gibco #17701-038)
Hepatocyte Wash Medium	Supplemented with 5ml penicillin-streptomycin (100x). (Gibco #17704-024)
William's E Medium	Supplemented with 5-10% FBS, 5ml Glutamax, Dexamethasone, Insulin, 5ml penicillin-streptomycin (100x) and GA-100. (Gibco #A12176-01)

Table 5. Orfan Biotech recommendation of Mediums from Gibco Life Technologies.

A 10x 20x

WT. Pre plated (hematocytometer)

B 10x 20x 40x

———— WT. 20h after plated ————

C 10x 20x 40x

———— WT. 22h after médium replacement ————

D 10x 20x 40x

———— WT. 22h after Starvation Medium ————

Figure 12. Hepatocyte isolation results after following *Orfan Biotech* instructions. (A) Wild type hepatocytes pre-plated in hematocytometer. (B) Same hepatocytes 20h after plated in William's E Medium. All cells in suspension are dead cell. (C) 22h after William's E Medium replacement. (D) 22h after Starvation Medium replacement.

In order to further characterize the cultured hepatocytes, a bibliographic research for specific markers was performed, with the goal to apply those markers to our cultures. The research for biomarkers in rodent's livers to differentiate primary hepatocytes in culture, has been challenging and studied for a long time. There are different markers and signals that can ensure cell identity and the functionality of hepatocytes. For instance, albumin and fibrinogen proteins are secreted by cultured hepatocytes to the medium, and they present CYP3A4 enzymatic activity. Primary hepatocytes stain positive to the liver-specific surface marker ASGR1, and they also highly express the following markers: ATT, CPS1, albumin, FAH, HGD and the hepatic asialoglycoprotein receptor (ASGPR) (Severgnini, Sherman et al. 2012, Ang, Tan et al. 2018). The use of some of these markers to characterize our cultures was precluded by the onset of the sanitary crisis.

Glucose production in cultured primary hepatocytes

To set up the glucose production assay in wild type and Tg.sgk1 hepatocytes, we used cell supernatants after incubation with or without induction media for 24h (Table 1) in cultures obtained from two livers (one from each genotype). Our preliminary data suggests that glucose production in wild type hepatocytes increases from non-induced to induced conditions by approximately 25% (Figure 13A). Under basal conditions, Tg.sgk1 hepatocytes produce insignificant amounts of glucose, although treatment with induction medium results in detectable glucose in the medium (Figure 13A). The different result obtained with wild type and Tg.sgk1 hepatocytes could be explained by different number of cells in each culture. Therefore, glucose concentration was normalized to total RNA obtained from cells in each well, which was assumed to represent the amount of cells in culture, since it resulted to be more precise than protein quantification (Figure 13B).

However, the normalization did not significantly alter the results, which appear to contradict our hypothesis. However, additional experiments with larger number of mice, and hepatocytes per mouse, are needed to reach a definitive conclusion.
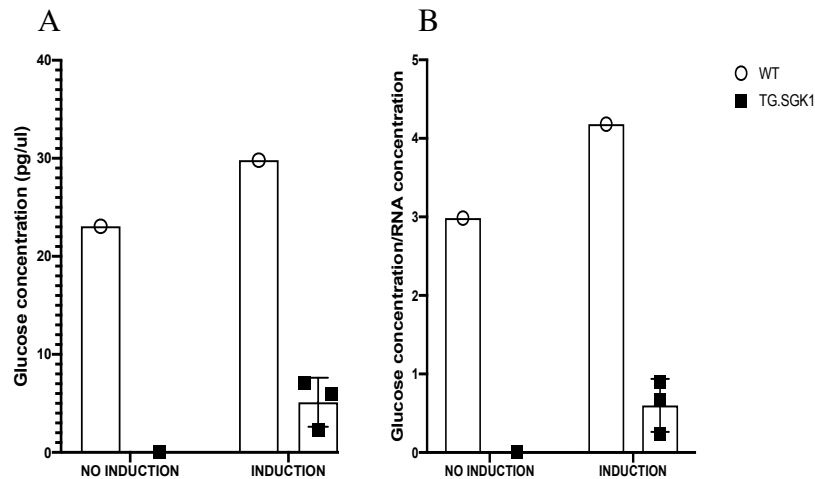

Figure 13. Glucose Production Assay. (A) Glucose concentration in wild type and Tg.sgk1 hepatocytes. (B) Glucose concentration normalized with its RNA concentration.

Influence of SGK1 on the expression of gluconeogenesis and glucose transport markers in mouse liver

There is strong evidence supporting hyperglycemia in Tg.sgk1 mice during the fasting state (Sierra-Ramos, Velazquez-Garcia et al. 2020), which together with the PTT assays performed in these mice (Figure 5) suggests an increase of glucose production in the liver. Therefore, we compared the expression of two key gluconeogenesis enzymes (PCK1 and G6Pc) and a glucose transporter (GLUT2) in WT and Tg.sgk1 animals in normal conditions and after 24h fasting, which should induce the expression of gluconeogenesis markers.

Our data comparing the relative mRNA expression of these three markers under normal diet in WT and transgenic animals showed a significantly increased expression of G6Pc (Figure 14), which supports the hypothesis of

SGK1 abnormally increasing gluconeogenesis under basal conditions. Surprisingly, fasting failed to increased gluconeogenesis markers in both genotypes and even decreased G6Pc expression in Tg.sgk1 (Figure 14). This is an unexpected result, since it has bene previously described that gluconeogenesis genes are transcriptionally upregulated during fasting (Goldstein, Baek et al. 2017). There were no significant differences in GLUT2 expression between genotypes, although fasting reduced the expression of this transporter (Figure 14). GLUT2 is the major glucose transporter in mouse hepatocytes and is responsible for glucose release to the blood stream during fasting. However, deletion of GLUT2 in mice does not affect glucose homeostasis during the fasting or fed state, indicating that alternative pathways exist for the entry and exit of glucose in hepatocytes (Burcelin, del Carmen Munoz et al. 2000).
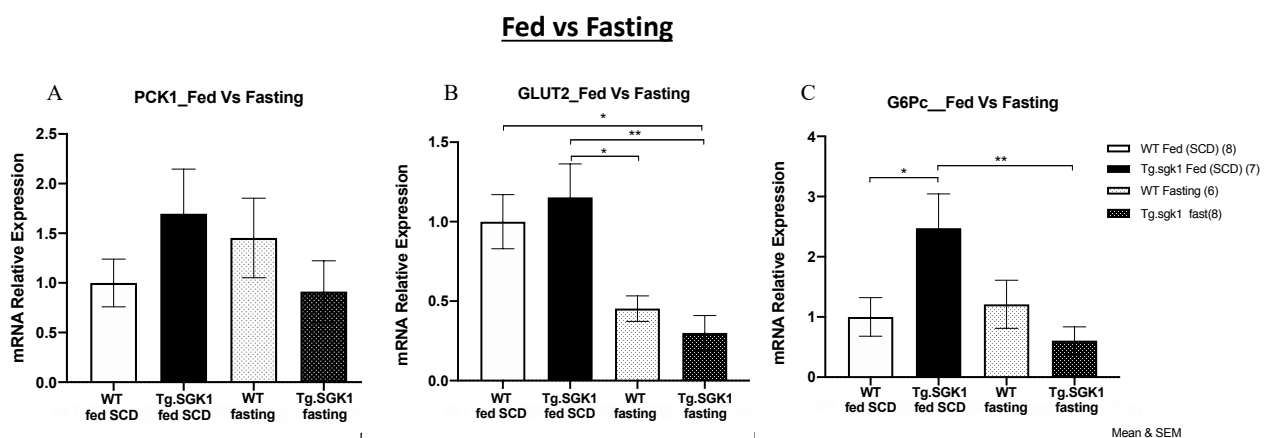
Fed vs Fasting

Figure 14. mRNA relative expression. (A) PCK1 mRNA relative expression compared to the basal state (fed with SCD). (B) GLUT2 mRNA relative expression compared to the basal state (fed with SCD). (C) G6PC mRNA relative expression compared to the basal state (fed with SCD).

In addition to studying mRNA expression, we measured PCK1 and GLUT2 protein abundance in liver extracts from WT and Tg.sgk1 mice. Suprinsingly, PCK1 expression was lower in Tg.sgk1 when compared to WT mice (Figure 15A). GLUT2 protein expression was unaffected by genotype or treatment (Figure 15B).
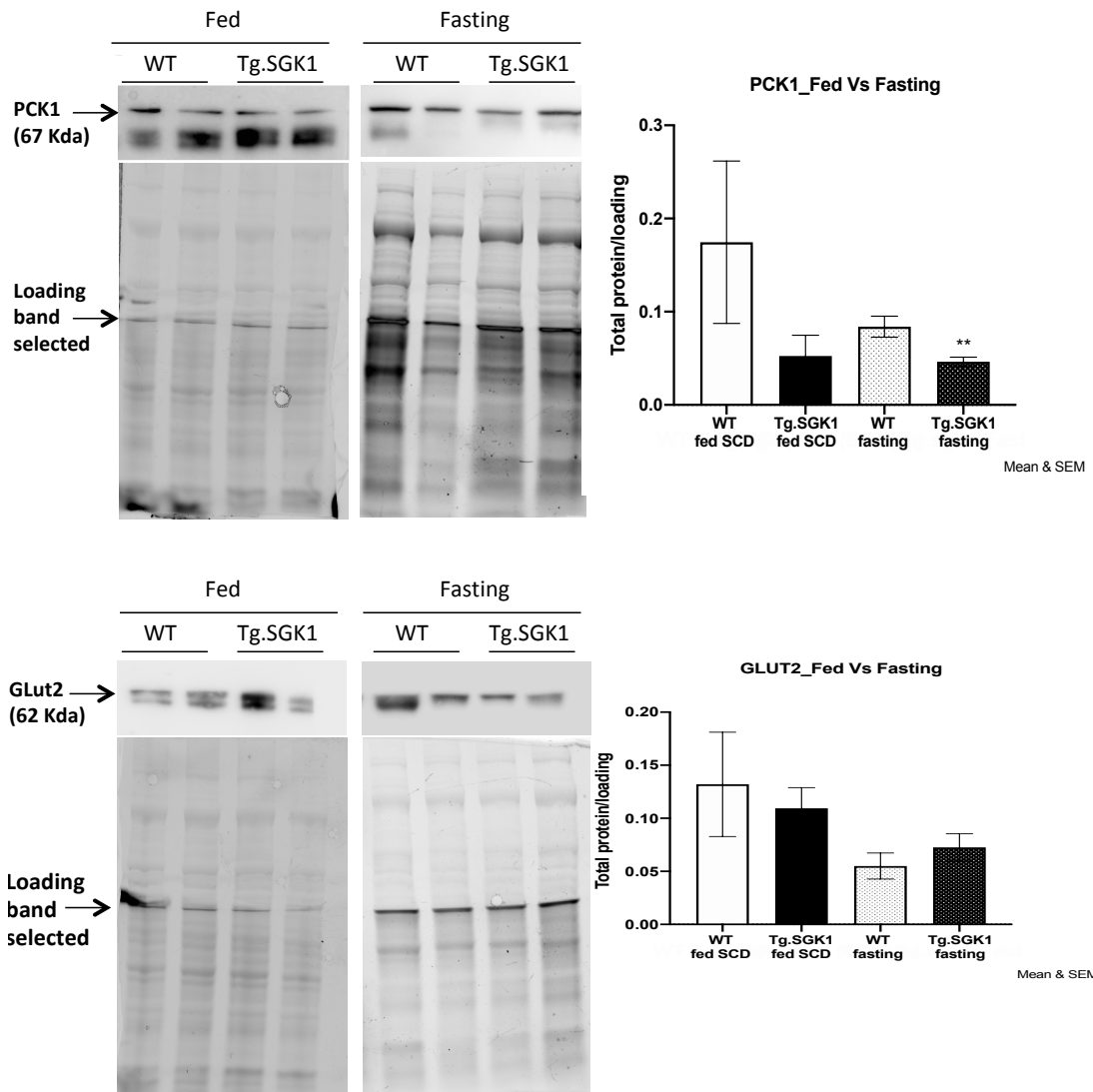
Figure 15. PCK1 and GLUT2 total protein abundance in liver under fed or fasting conditions.

CONCLUSIONS

- The Hepatocyte Isolation protocol is still in need of further optimization to reduce the number of dead cells after the first 24h of culture.

- Additional experiments with larger number of mice, and hepatocytes per mouse, are needed to reach a definitive conclusion about whether SGK1 has a direct effect in hepatocytes' glucose production.

- Expression of the gluconeogenesis markers in the liver does not increase during fasting, and in addition to GLUT2 expression decreasing, we assume that there must be alternative pathways for the transport of glucose in hepatocytes.

- PCK1 protein expression was lower in Tg.sgk1 than WT, and GLUT2 protein expression resulted unaffected by genotype or treatment.

- Due to the unexpected stop for the COVID-19, conclusive answers cannot be defined to our aims, and we look forward to keep researching in this investigation line.

Ackermann, T. F., K. M. Boini, N. Beier, W. Scholz, T. Fuchss and F. Lang (2011). "EMD638683, a novel SGK inhibitor with antihypertensive potency." Cell Physiol Biochem **28**(1): 137-146.

Alvarez de la Rosa, D. and C. M. Canessa (2003). "Role of SGK in hormonal regulation of epithelial sodium channel in A6 cells." Am J Physiol Cell Physiol **284**(2): C404-414.

Ang, L. T., A. K. Y. Tan, M. I. Autio, S. H. Goh, S. H. Choo, K. L. Lee, J. Tan, B. Pan, J. J. H. Lee, J. J. Lum, C. Y. Y. Lim, I. K. X. Yeo, C. J. Y. Wong, M. Liu, J. L. L. Oh, C. P. L. Chia, C. H. Loh, A. Chen, Q. Chen, I. L. Weissman, K. M. Loh and B. Lim (2018). "A Roadmap for Human Liver Differentiation from Pluripotent Stem Cells." Cell Rep **22**(8): 2190-2205.

Armas-Capote, N., L. E. Maglio, L. Perez-Atencio, E. Martin-Batista, A. Reboreda, J. A. Barios, G. Hernandez, D. Alvarez de la Rosa, J. A. Lamas, L. C. Barrio and T. Giraldez (2020). "SGK1.1 Reduces Kainic Acid-Induced Seizure Severity and Leads to Rapid Termination of Seizures." Cereb Cortex **30**(5): 3184-3197.

Arteaga, M. F., D. Alvarez de la Rosa, J. A. Alvarez and C. M. Canessa (2007). "Multiple translational isoforms give functional specificity to serum- and glucocorticoid-induced kinase 1." Mol Biol Cell **18**(6): 2072-2080.

Brunet, A., J. Park, H. Tran, L. S. Hu, B. A. Hemmings and M. E. Greenberg (2001). "Protein kinase SGK mediates survival signals by phosphorylating the forkhead transcription factor FKHRL1 (FOXO3a)." Mol Cell Biol **21**(3): 952-965.

Burcelin, R., M. del Carmen Munoz, M. T. Guillam and B. Thorens (2000). "Liver hyperplasia and paradoxical regulation of glycogen metabolism and glucose-sensitive gene expression in GLUT2-null hepatocytes. Further evidence for the existence of a membrane-based glucose release pathway." J Biol Chem **275**(15): 10930-10936.

Calabuig-Navarro, V., J. Yamauchi, S. Lee, T. Zhang, Y. Z. Liu, K. Sadlek, G. M. Coudriet, J. D. Piganelli, C. L. Jiang, R. Miller, M. Lowe, H. Harashima and H. H. Dong (2015). "Forkhead Box O6 (FoxO6) Depletion Attenuates Hepatic Gluconeogenesis and Protects against Fat-induced Glucose Disorder in Mice." J Biol Chem **290**(25): 15581-15594.

Chu, S., S. Rushdi, E. T. Zumpe, P. Mamers, D. L. Healy, T. Jobling, H. G. Burger and P. J. Fuller (2002). "FSH-regulated gene expression profiles in ovarian tumours and normal ovaries." Mol Hum Reprod **8**(5): 426-433.

Chung, E. J., Y. K. Sung, M. Farooq, Y. Kim, S. Im, W. Y. Tak, Y. J. Hwang, Y. I. Kim, H. S. Han, J. C. Kim and M. K. Kim (2002). "Gene expression profile analysis in human hepatocellular carcinoma by cDNA microarray." Mol Cells **14**(3): 382-387.

Di Cristofano, A. (2017). "SGK1: The Dark Side of PI3K Signaling." Curr Top Dev Biol **123**: 49-71.

Firestone, G. L., J. R. Giampaolo and B. A. O'Keeffe (2003). "Stimulus-dependent regulation of serum and glucocorticoid inducible protein kinase (SGK) transcription, subcellular localization and enzymatic activity." Cell Physiol Biochem **13**(1): 1-12.

Fujita, T. (2008). "Aldosterone in salt-sensitive hypertension and metabolic syndrome." J Mol Med (Berl) **86**(6): 729-734.

Garcia-Martinez, J. M. and D. R. Alessi (2008). "mTOR complex 2 (mTORC2) controls hydrophobic motif phosphorylation and activation of serum- and glucocorticoid-induced protein kinase 1 (SGK1)." Biochem J **416**(3): 375-385.

Goldstein, I., S. Baek, D. M. Presman, V. Paakinaho, E. E. Swinstead and G. L. Hager (2017). "Transcription factor assisted loading and enhancer dynamics dictate the hepatic fasting response." Genome Res **27**(3): 427-439.

Huang, P. L. (2009). "A comprehensive definition for metabolic syndrome." Dis Model Mech **2**(5-6): 231-237.

Kaur, J. (2014). "A comprehensive review on metabolic syndrome." Cardiol Res Pract **2014**: 943162.

Klaunig, J. E., P. J. Goldblatt, D. E. Hinton, M. M. Lipsky, S. M. Knipe and B. F. Trump (1982). "Morphologic and functional studies of mouse hepatocytes in primary culture." Anat Rec **204**(3): 231-243.

Kobayashi, T. and P. Cohen (1999). "Activation of serum- and glucocorticoid-regulated protein kinase by agonists that activate phosphatidylinositide 3-kinase is mediated by 3-phosphoinositide-dependent protein kinase-1 (PDK1) and PDK2." Biochem J **339 (Pt 2)**: 319-328.

Lang, F., F. Artunc and V. Vallon (2009). "The physiological impact of the serum and glucocorticoid-inducible kinase SGK1." Curr Opin Nephrol Hypertens **18**(5): 439-448.

Lang, F., C. Bohmer, M. Palmada, G. Seebohm, N. Strutz-Seebohm and V. Vallon (2006). "(Patho)physiological significance of the serum- and glucocorticoid-inducible kinase isoforms." Physiol Rev **86**(4): 1151-1178.

Lang, F., N. Strutz-Seebohm, G. Seebohm and U. E. Lang (2010). "Significance of SGK1 in the regulation of neuronal function." J Physiol **588**(Pt 18): 3349-3354.

Li, P., Y. Hao, F. H. Pan, M. Zhang, J. Q. Ma and D. L. Zhu (2016). "SGK1 inhibitor reverses hyperglycemia partly through decreasing glucose absorption." J Mol Endocrinol **56**(4): 301-309.

Li, W. C., K. L. Ralphs and D. Tosh (2010). "Isolation and culture of adult mouse hepatocytes." Methods Mol Biol **633**: 185-196.

Liu, H., J. Yu, T. Xia, Y. Xiao, Q. Zhang, B. Liu, Y. Guo, J. Deng, Y. Deng, S. Chen, A. Naray-Fejes-Toth, G. Fejes-Toth and F. Guo (2014). "Hepatic serum- and glucocorticoid-regulated protein kinase 1 (SGK1) regulates insulin sensitivity in mice via extracellular-signal-regulated kinase 1/2 (ERK1/2)." Biochem J **464**(2): 281-289.

Lou, Y., F. Zhang, Y. Luo, L. Wang, S. Huang and F. Jin (2016). "Serum and Glucocorticoid Regulated Kinase 1 in Sodium Homeostasis." Int J Mol Sci **17**(8).

Mason, J. A., J. A. Cockfield, D. J. Pape, H. Meissner, M. Sokolowski, T. C. White, J. C. Valentín López, J. Liu, X. Liu, I. Martínez-Reyes, N. S. Chandel, J. W. Locasale and Z. T. Schafer (2020). "SGK1 Signaling Promotes Glucose Metabolism and Survival in Extracellular Matrix Detached Cells." bioRxiv: 2020.2003.2020.000463.

Murray, J. T., D. G. Campbell, N. Morrice, G. C. Auld, N. Shpiro, R. Marquez, M. Peggie, J. Bain, G. B. Bloomberg, F. Grahammer, F. Lang, P. Wulff, D. Kuhl and P. Cohen (2004). "Exploitation of KESTREL to identify NDRG family members as physiological substrates for SGK1 and GSK3." Biochem J **384**(Pt 3): 477-488.

Overturf, K., M. Al-Dhalimy, M. Finegold and M. Grompe (1999). "The repopulation potential of hepatocyte populations differing in size and prior mitotic expansion." Am J Pathol **155**(6): 2135-2143.

Petersen, M. C., D. F. Vatner and G. I. Shulman (2017). "Regulation of hepatic glucose metabolism in health and disease." Nat Rev Endocrinol **13**(10): 572-587.

Radonic, A., S. Thulke, I. M. Mackay, O. Landt, W. Siegert and A. Nitsche (2004). "Guideline to reference gene selection for quantitative real-time PCR." Biochem Biophys Res Commun **313**(4): 856-862.

Rauhala, H. E., K. P. Porkka, T. T. Tolonen, P. M. Martikainen, T. L. Tammela and T. Visakorpi (2005). "Dual-specificity phosphatase 1 and serum/glucocorticoid-regulated kinase are downregulated in prostate cancer." Int J Cancer **117**(5): 738-745.

Rubie, C., K. Kempf, J. Hans, T. Su, B. Tilton, T. Georg, B. Brittner, B. Ludwig and M. Schilling (2005). "Housekeeping gene variability in normal and cancerous colorectal, pancreatic, esophageal, gastric and hepatic tissues." Mol Cell Probes **19**(2): 101-109.

Rui, L. (2014). "Energy metabolism in the liver." Compr Physiol **4**(1): 177-197.

Saisho, Y. (2015). "Metformin and Inflammation: Its Potential Beyond Glucose-lowering Effect." Endocr Metab Immune Disord Drug Targets **15**(3): 196-205.

Saklayen, M. G. (2018). "The Global Epidemic of the Metabolic Syndrome." Curr Hypertens Rep **20**(2): 12.

Satoh, N., M. Nakamura, M. Suzuki, A. Suzuki, G. Seki and S. Horita (2015). "Roles of Akt and SGK1 in the Regulation of Renal Tubular Transport." Biomed Res Int **2015**: 971697.

Severgnini, M., J. Sherman, A. Sehgal, N. K. Jayaprakash, J. Aubin, G. Wang, L. Zhang, C. G. Peng, K. Yucius, J. Butler and K. Fitzgerald (2012). "A rapid two-step method for isolation of functional primary mouse hepatocytes: cell characterization and asialoglycoprotein receptor based assay development." Cytotechnology **64**(2): 187-195.

Sierra-Ramos, C., S. Velazquez-Garcia, A. Vastola-Mascolo, G. Hernandez, N. Faresse and D. Alvarez de la Rosa (2020). "SGK1 activation exacerbates diet-induced obesity, metabolic syndrome and hypertension." J Endocrinol **244**(1): 149-162.

Vallon, V., D. Y. Huang, F. Grahammer, A. W. Wyatt, H. Osswald, P. Wulff, D. Kuhl and F. Lang (2005). "SGK1 as a determinant of kidney function and salt intake in response to mineralocorticoid excess." Am J Physiol Regul Integr Comp Physiol **289**(2): R395-R401.

von Wowern, F., G. Berglund, J. Carlson, H. Mansson, B. Hedblad and O. Melander (2005). "Genetic variance of SGK-1 is associated with blood pressure, blood pressure change over time and strength of the insulin-diastolic blood pressure relationship." Kidney Int **68**(5): 2164-2172.

Voskas, D., L. S. Ling and J. R. Woodgett (2010). "Does GSK-3 provide a shortcut for PI3K activation of Wnt signalling?" F1000 Biol Rep **2**: 82.

Waldegger, S., P. Barth, G. Raber and F. Lang (1997). "Cloning and characterization of a putative human serine/threonine protein kinase transcriptionally modified during anisotonic and isotonic alterations of cell volume." Proc Natl Acad Sci U S A **94**(9): 4440-4445.

Webster, M. K., L. Goya, Y. Ge, A. C. Maiyar and G. L. Firestone (1993). "Characterization of sgk, a novel member of the serine/threonine protein kinase gene family which is transcriptionally induced by glucocorticoids and serum." Mol Cell Biol **13**(4): 2031-2040.

Yan, L., V. Mieulet and R. F. Lamb (2008). "mTORC2 is the hydrophobic motif kinase for SGK1." Biochem J **416**(3): e19-21.

Yang, K., Z. Chen, J. Gao, W. Shi, L. Li, S. Jiang, H. Hu, Z. Liu, D. Xu and L. Wu (2017). "The Key Roles of GSK-3beta in Regulating Mitochondrial Activity." Cell Physiol Biochem **44**(4): 1445-1459.